

***POMPUS: an optimized EIT reconstruction
algorithm***

Paulson, K and Lionheart, W and Pidcock, M

1995

MIMS EPrint: **2015.44**

Manchester Institute for Mathematical Sciences
School of Mathematics

The University of Manchester

Reports available from: <http://eprints.maths.manchester.ac.uk/>

And by contacting: The MIMS Secretary
School of Mathematics
The University of Manchester
Manchester, M13 9PL, UK

ISSN 1749-9097

POMPUS: an optimized EIT reconstruction algorithm

Kevin Paulson, William Lionheart and Michael Pidcock

School of Computing and Mathematical Sciences, Oxford Brookes University, Oxford
OX3 0BP, UK

Received 11 February 1994, in final form 26 October 1994

Abstract. Electrical impedance tomography (EIT) is a non-invasive imaging technique which aims to image the impedance of material within a test volume from electrical measurements made on the surface. The reconstruction of impedance images is an ill-posed problem which is both extremely sensitive to noise and highly computationally intensive. This paper defines an experimental measurement in EIT and calculates optimal experiments which maximize the distinguishability between the region to be imaged and a best estimate conductivity distribution. These optimal experiments can be derived from measurements made on the boundary. We describe a reconstruction algorithm, known as POMPUS, which is based on the use of optimal experiments. We have shown that, given some mild constraints, if POMPUS converges, it converges to a stationary point of our objective function. It is demonstrated to be many times faster than standard, Newton based, reconstruction algorithms. Results using synthetic data indicate that the images produced by POMPUS are comparable to those produced by these standard algorithms.

1. Introduction

Electrical impedance tomography (EIT) is a non-invasive imaging technique with widespread applications in medicine and industry. It aims to image the conductivity distribution within a test volume by making electrical measurements on the surface of the volume. Typically this involves injecting current through electrodes attached to the surface and measuring the induced voltage on other, or possibly the same, electrodes. The technique has advantages over other functional medical imaging techniques, such as MRI, emission and radiative imaging, of being fast, inexpensive, portable and relatively harmless but it also has the disadvantage of poor image resolution. The electrode voltages induced by the application of currents are a highly nonlinear function of the conductivity distribution. Consequently, inversion of the current–voltage data to produce an image of the conductivity distribution is often performed using an iterative process. Breckon and Pidcock [3, 4] describe an iterative, full matrix method for the inversion of EIT data.

Iterative reconstruction techniques proceed by comparing a set of voltage measurements predicted by a model using an assumed conductivity distribution with physical measurements made on the volume to be imaged. At each iteration the model conductivity distribution is updated to reduce some measure of the difference between the two sets of measurements. Both of these stages in reconstruction are computationally intensive. The amount of computation and the effectiveness of an iteration are strongly determined by the experimental measurements used for reconstruction. It is important to make the measurements which minimize the computation and which yield the most information upon which to base the reconstruction.

2. Experimental measurements in EIT

In EIT, a volume Ω with boundary $\partial\Omega$ and unknown conductivity distribution σ is imaged by applying electric current to a finite number of electrodes fixed to the boundary. Within a source free conductor the potential ϕ is governed by the equation:

$$\nabla \cdot \sigma \nabla \phi = 0 \quad \text{in } \Omega.$$

This is a second-order partial differential equation in ϕ which, for arbitrary conductivity distributions, can only be solved numerically. In the quasi-static case for alternating currents, the potential and conductivity can be complex. For a unique solution to exist a complete set of boundary conditions needs to be known. These may be Dirichlet conditions in the form of potentials on the boundary, Neumann conditions in the form of current densities on the boundary or a combination of both. There must be at least one constraint on the potential for a unique solution to exist. The boundary conditions associated with the injection of current through a finite number of electrodes are explored in Cheng *et al* [6] and Paulson *et al* [13]. In EIT the inverse problem is solved; the conductivity distribution σ is calculated from knowledge of the currents injected into the region and measurements of the boundary voltages.

The voltage, V , induced on the boundary of a region with conductivity σ can be expressed in terms of the transfer impedance operator, $R(\sigma)$, acting on the applied current pattern, J , by the equation $V = R(\sigma)J$. To include all current patterns of finite power the transfer impedance operator acts on current patterns in the Sobolev space $H^{-1/2}$ and yields voltage patterns in the space $H^{+1/2}$. If the transfer impedance operator is restricted to $R(\sigma): H^0 \rightarrow H^0$, it is self-adjoint and compact and, thus, not continuously invertible.

As there are no sources or sinks in the interior of the region, the net current crossing the boundary is zero. This is a constraint on the current patterns we can apply. Similarly, as the potential is only defined up to an additive constant we can eliminate the ambiguity so that the average potential on the boundary is zero. This is a constraint on the voltage patterns we can measure. These constraints remove one dimension from the spaces of current and voltage patterns. Thus, for quantities defined on the boundary, H^s is understood to be the subspace of H^s orthogonal to 1.

If the boundary voltage and current patterns are approximated in bases of functions, $\{\chi_i\} \subset H^{+1/2}$ and $\{\xi_i\} \subset H^{-1/2}$ respectively, then the transfer impedance operator can be represented as a matrix:

$$V = R(\sigma)J$$

where

$$(R(\sigma))_{ij} = \langle \chi_i, R(\sigma)\xi_j \rangle.$$

We shall be considering finite dimensional subspaces spanned by the first n and m of these functions respectively. The domain and range of the transfer impedance matrix are the spaces spanned by the bases for the current and voltage patterns. If $\chi_i = \xi_i$, $i = 1, \dots, m = n$ then the restricted transfer impedance matrix is self-adjoint.

If the bases are orthonormal and orthogonal to 1, i.e.

$$\langle \chi_i, \chi_j \rangle = \langle \xi_i, \xi_j \rangle = \delta_{ij} \quad \text{and} \quad \langle \chi_i, 1 \rangle = \langle \xi_i, 1 \rangle = 0$$

then the dual pairing of two functions, F and G , approximated in the same basis may be written as a vector dot product, $\langle F, G \rangle = F \cdot G$. If F and G are both smooth functions then

$$\langle F, G \rangle = \int_{\partial\Omega} \bar{F} G.$$

A full description of Sobolev spaces and dual pairings is given in Folland [8].

For real EIT systems, currents are applied and voltages are measured via electrodes attached to the boundary of the region. If current is applied through m electrodes and voltage is measured on n electrodes then the transfer impedance matrix can be defined using a current and voltage basis function associated with each electrode:

$$V = R(\sigma)I.$$

If $n = m$ then the matrix is invertible. The transfer impedance matrix belongs to a space of complex matrices. $R(\sigma) \in C^{(m-1) \times (n-1)}$. $V \in C^{(n-1)}$ and $I \in C^{(m-1)}$ are vectors of the voltages and currents measured on the electrodes. The current and voltage on the last current driving and voltage measuring electrodes are determined via the constraints:

$$\sum_{i=1}^m I_i = \sum_{i=1}^n V_i = 0.$$

If current and voltage are measured on different sets of electrodes the transfer impedance matrix need not be square and is not symmetric. Under special conditions, see Somersalo *et al* [16], the transfer impedance matrix may be self-adjoint if measurements are made on the same set of electrodes.

An experiment in EIT can be defined as a measurement of a component of the difference between the voltage pattern induced on the surface of the region to be imaged and that predicted by a numerical model, by the application of a current pattern to the surface. Each experimental measurement involves the application of a current pattern to the boundary of the region. A component of the resultant boundary voltage pattern is measured with respect to a particular basis of the space of measurements. An experimental measurement thus results in a single number:

$$E_{ij}(\sigma_m) = \langle M_i, D(\sigma_m)J_j \rangle \quad (1)$$

where σ_m is the model conductivity distribution, σ_e is the test volume conductivity distribution, $R(\sigma)$ is the transfer impedance operator, $D(\sigma_m) = R(\sigma_m) - R(\sigma_e)$ is the difference in the transfer impedance operators, M_i is a measurement pattern, J_j is an applied current pattern, $\langle \cdot, \cdot \rangle$ is the appropriate dual pairing, Ω is the volume to be imaged and $\partial\Omega$ is its boundary.

The subscripts i and j on the measurement and current patterns range over the patterns used. The number of independent experiments will be determined by the number and position of electrodes used to apply current to the region and the number used to make voltage measurements on the region.

Three different forms of current pattern, J_j , are in common use. The back projection reconstruction algorithm of Barber and Brown [1, 2] assumes current patterns approximating dipoles on the surface. Their APT current patterns achieve this by driving current through adjacent electrodes attached to the surface. Isaacson [12] derived an algorithm for

calculating optimal current patterns which maximize the norm of the difference between the voltages measured on the region to be imaged and those predicted by the numerical model. These current patterns vary smoothly around the surface of the region and are approximated by driving current through all the electrodes simultaneously. Some researchers, including Isaacson and our group at Oxford Brookes University, have used trigonometric current patterns, $I_i^{\text{trig}} = \cos(k\theta_i)$ or $\sin(k\theta_i)$ $k = 1, 2, 3, \dots$, where I_i^{trig} is the current on the i th electrode and θ_i is its angular position.

All other researchers known to this group use measurement patterns corresponding to measuring the voltage between pairs of electrodes. Most groups measure the voltage difference between adjacent electrodes. In this paper we consider trigonometric measurements and optimal measurements defined in section 3. In practice, smooth measurement patterns, such as trigonometric and optimal measurements, are calculated from a linear combination of voltage measurements made between pairs of electrodes. Thus, these measurements have a larger noise component than the physical measurements made between pairs of electrodes. Unless this noise component becomes very large, the benefits of using measurement patterns and the POMPUS algorithm described in section 4 outweigh the small increase in the noise in the data. Paulson *et al* [15] consider current patterns optimized for voltage measurements between pairs of electrodes.

3. Optimal experimental measurements

A set of experimental measurements is the data used to calculate the update to the model conductivity; $\sigma_m \rightarrow \sigma_m + \Delta\sigma$. The update, $\Delta\sigma$, is chosen so as to minimize a measure of the size of D , the difference in the transfer impedance matrices, such as the Frobenius norm of D :

$$\|D\|_F^2 = \sum_{i=1}^m \sum_{j=1}^n E_{ij}^2(\sigma_m).$$

An important question is: ‘What are the best experiments to perform?’ For measurements with a background random error of fixed amplitude, such as thermal or digital quantization noise, the measurements of highest precision are those for which E_{ij} is largest. Clearly, experimental measurements which are small compared to the background noise yield little information upon which to base a reconstruction. Following the work of Isaacson [12] it is instructive to find which experimental measurements maximize the distinguishability between the two regions.

An understanding of the relationship between current and measurement patterns and the resulting experimental measurements can be gained by considering the singular value decomposition, SVD, of the difference in the transfer impedance operators. The SVD of operators is described in detail in Groetsch [10], and the SVD of matrices is described in Golub and Van Loan [9]. There exist functions, U_i and V_i , and positive real numbers λ_i such that

$$\begin{aligned} DU_i &= \lambda_i V_i & D^*V_i &= \lambda_i U_i \\ \lambda_i &\geq \lambda_j \geq 0 & \forall i < j & \quad \langle U_i, U_j \rangle = \langle V_i, V_j \rangle = \delta_{ij} \end{aligned}$$

where D^* is the adjoint of D . The U_i s and the V_i s are the right and left singular functions of $D(\sigma_m)$ and form orthonormal bases for the space of applicable current patterns and voltage

patterns respectively. The λ_i s are singular values of the current to voltage difference map. Equation (1) can be rewritten in terms of this singular decomposition: since

$$J_j = \sum_k \langle U_k, J_j \rangle U_k$$

we see that

$$E_{ij} = \left\langle M_i, \sum_k V_k \lambda_k \langle U_k, J_j \rangle \right\rangle = \sum_k \langle M_i, V_k \rangle \lambda_k \langle U_k, J_j \rangle. \quad (2)$$

If $M_i = V_i$ and $J_j = U_j$ then the experimental measurement made using the i th singular measurement pattern and the j th singular current pattern is

$$E_{ij} = \sum_k \langle V_i, V_k \rangle \lambda_k \langle U_k, U_j \rangle = \lambda_i \delta_{ij}. \quad (3)$$

It is clear from this that the ‘best’ experimental measurement that can be made, meaning the one that produces the largest number, is E_{11} , the next best is E_{22} etc. All E_{ij} with $i \neq j$ are zero. Using the discrete quantities, equation (2) may be written more concisely as

$$E_{ij} = M_i^* V \Lambda U^* J_j$$

where U and V are basis matrices in which the columns are orthonormal vectors and $\Lambda = \text{Diag}(\lambda_1, \lambda_2, \lambda_3, \dots, \lambda_{\min(m,n)-1})$.

Isaacson *et al* [12] define the *distinguishability* between two conductivity distributions, $\delta(J)$, as

$$\delta(J) = \frac{\|DJ\|_0}{\|J\|_0}$$

and the ‘best’ current patterns in terms of maximizing the distinguishability as the eigenfunctions of the restricted, self-adjoint operator $|D|: H^0 \rightarrow H^0$. $|D|$ is the operator with eigenvalues that are the modulus of the eigenvalues of D . If the SVD is performed on the restricted operator then

$$|D|J = \sum_k U_k \lambda_k \langle U_k, J \rangle.$$

It is clear that the U_i s are eigenfunctions of this operator and so Isaacson’s optimal current patterns are the same as those calculated earlier in this section. The analysis using the SVD has the advantage that it makes clear the properties of different voltage measurement schemes and has led to the development of more efficient reconstruction algorithms.

4. Reconstruction algorithms

Newton-based reconstruction algorithms improve the initial estimates of the conductivity distribution by finding the least-squares solution to linearized forms of the inverse problem:

$$J\Delta\sigma = E \quad (4)$$

where \mathbf{E} is a vector of experimental measurements and $\mathbf{J} = [\partial E/\partial s]$ is the Jacobian matrix with elements that are the derivatives of the measurements with respect to the model conductivity parametrization. The conductivity and the conductivity update are expressed in a finite basis of continuous functions B_i , $\Delta\sigma = \sum \Delta s_i B_i = \Delta s \cdot \mathbf{B}$. Thus the ij, k th element of this matrix is $\partial E_{ij}/\partial s_k$ where ij indexes the experimental measurement made using the i th measurement pattern and the j th current pattern. Any selection of experimental measurements may be used for reconstruction.

RECON is a typical, regularized, adaptive reconstruction algorithm developed by our group at Oxford. It applies trigonometric current patterns and the measurement patterns are fixed to be either trigonometric or adjacent electrode pair measurements. The number of experimental measurements used for reconstruction is determined by the number and location of the electrodes used for current driving and voltage measurement. Typically, the number of experimental measurements used will be $(m-1)(n-1)$ where n and m are the number of current driving and voltage measuring electrodes respectively. Not all of these experimental measurements will be independent. The number of conductivity parameters which can be determined will be less, therefore, than the number of independent experimental measurements used for reconstruction. The RECON algorithm can be described schematically as

RECON

WHILE $\mathbf{E}^T \mathbf{E} > \varepsilon$ DO

- measure $R(\sigma_m)$
- calculate $D(\sigma_m)$ and hence calculate optimal \mathbf{J}_j
- make the measurements $E_{ij}: 1 \leq i \leq n-1, 1 \leq j \leq m-1$
- find the regularized least-squares solution to (4)

$$\Delta s = (\mathbf{J}_r^* \mathbf{J}_r + \mu^2 I)^{-1} \mathbf{J}_r^* \mathbf{E}$$

ENDWHILE.

The least-squares system is regularized by the addition of $\mu^2 I$, the Tikhonov factor multiplied by the identity matrix. The computational cost of solving the least-squares system increases as the cube of the dimension of the RECON Jacobian matrix \mathbf{J}_r . For a system that drives current and makes voltage measurements on the same set of n electrodes the number of independent measurements that can be made is $n(n-1)/2$, or less with some symmetries. This figure is essentially half the number of independent current patterns multiplied by the number of independent measurement patterns as a consequence of the reciprocity theorem [4]. This sets a limit on the number of conductivity parameters that can be imaged with a given system of electrodes. For typical electrode configurations the number of independent measurements that can be made is $O(n^2)$ and so the computational cost of solving the least squares system is $O((n^2)^3) = O(n^6)$.

The authors propose an algorithm, that has come to be known as POMPUS, to circumvent this staggering increase in computational cost with increasing numbers of electrodes and resolution. The method is based on the use of the optimal current and measurement patterns defined in section 3. The major advantage of this algorithm is the reduction in the size of system (4) from $O(n^2)$ to $O(n)$ and so the computational cost is reduced from $O(n^6)$ to $O(n^3)$. This is accomplished by not including the equations for experimental measurements $E_{ij}: i \neq j$ in equation (4) and hence using a much smaller POMPUS Jacobian matrix, \mathbf{J}_p . The algorithm can be stated as

POMPUS

WHILE $E_{11} > \varepsilon$ DO

- measure $R(\sigma_m)$
- calculate $D(\sigma_m)$ and hence calculate optimal M_i and J_j
- make the measurements $E_{ii}: E_{ii} > \varepsilon$
- find the regularized least-squares solution to (4) for experimental measurements $E_{ii}: E_{ii} > \varepsilon$ using

$$\Delta s = \mathbf{J}_p^* (\mathbf{J}_p \mathbf{J}_p^* + \mu^2 I)^{-1} E$$

- $\sigma_m \rightarrow \sigma_m + \Delta \sigma$

ENDWHILE.

In RECON the Jacobian system, equation (4) is overdetermined and the conductivity update is the one which best fits the experimental measurements. By contrast, in POMPUS, the Jacobian system is underdetermined and so the least-squares solution is the consistent conductivity update with the minimum norm.

It is not clear whether this algorithm will converge. A conductivity update which reduces the size of the experimental measurements E_{ii} could introduce larger variation into the, much more numerous, experimental measurements $E_{ij}, i \neq j$. This issue is discussed further in the next section.

5. Convergence of reconstruction algorithms

For a convergent reconstruction algorithm with exact data, the norm of the difference in the transfer impedance operators tends to a local minimum of the function $\|D(\sigma_m)\|$ or to the global minimum, $\|D(\sigma_m)\| = 0$, where no experimental measurements can distinguish the model and experimental conductivity distributions. Typically there will be some noise level, ε , within the measurement process. Conductivity updates calculated using experimental measurements smaller than ε are determined by the noise rather than the signal and consequently, reconstruction algorithms generally terminate if $\|D(\sigma_m)\| \leq \varepsilon$.

Recall that the steepest descent direction of a function G at the point x is $-\nabla G(x)$. A vector in a direction within 90° of the steepest descent direction is known as a descent direction. Iterative algorithms for minimizing a function, G , by repeatedly adding corrections along descent directions have been studied by Fletcher [7]. Fletcher gives conditions which, while not guaranteeing convergence, do ensure that an accumulation point of this sequence of approximations is a stationary point of the objective function. These conditions are that the gradient of G , ∇G , must be uniformly continuous on the level set $\{x: G(x) < G(x_0)\}$, where x_0 is the initial approximation of the position of the minimum, and the size of the update must satisfy the Wolfe–Powell conditions [7].

To show that the continuous objective function $G(\sigma_m) = \|D(\sigma_m)\|_F^2$ is uniformly continuous on level sets it is sufficient to show that the level sets are bounded. First note that the transfer impedance matrix, $R(\sigma)$, is positive definite and an analytic function of the conductivity parameters s_i , [5]. It also satisfies a positivity constraint; if $\sigma_1(x) > \sigma_2(x) \forall x \in \Omega$ then $R(\sigma_2) - R(\sigma_1)$ is positive definite. The model conductivity is parametrized in terms of N_b basis functions; $\sigma_m = \sigma_0 + \sum_{i=1}^{N_b} s_i b_i$ where σ_0 is a strictly positive constant and the basis functions are chosen to satisfy

$$\lim_{\eta \rightarrow \infty} R(\sigma_0 + \eta b_i) = 0.$$

Local bases, such as the finite element basis, do not satisfy this condition but any basis with $\inf(b_i) > 0$ does. From these conditions it can be shown that the objective function $\|D(\sigma_m)\|^2 \rightarrow \|R(\sigma_e)\|^2$ as $\|\sigma_m\| \rightarrow \infty$. For any $0 \leq K < \|R(\sigma_m)\|^2$ the level set $\{\sigma: \|D(\sigma)\|^2 < K\}$ is bounded and the objective function is uniformly continuous.

When $D(\sigma_m)$ is expressed in the optimal bases, defined by the matrices $U(\sigma_m)$ and $V(\sigma_m)$, it is a diagonal matrix, $D = \text{Diag}(E_{11}, E_{22}, \dots, E_{pp})$. When current and measurement patterns are expressed in these bases the optimal patterns are the standard basis vectors, e_i . Using these bases to define D allows the experimental measurements to be written $E_{ij} = e_i^* D e_j$. Thus as long as D is expressed in the local coordinate system defined by $U(\sigma_m)$ and $V(\sigma_m)$, the Frobenius norm of D is determined by its leading diagonal:

$$\|D(\sigma_m)\|_F^2 = \sum_{i=1}^p E_{ii}^2(\sigma_m).$$

Once a descent direction has been determined an update can be found which satisfies the Wolfe–Powell conditions in a finite number of steps. Thus, to show that any accumulation point of the reconstruction algorithm is stationary it is sufficient to show that the conductivity update is along a descent direction and to allow the appropriate amount of the update to be added at each iteration. In the remainder of this section it is shown that the POMPUS update is along a descent direction.

5.1. The steepest descent direction

The direction of steepest descent of the Frobenius norm of D , expressed in the singular bases, is

$$Z = -\nabla_s \|D(\sigma_m)\|_F^2 = -2 \sum_{i=1}^p E_{ii} \nabla_s E_{ii} = -2 \mathbf{J}_p^* E \quad (5)$$

where ∇_s is the gradient operator with respect to the conductivity parametrization. The Jacobian matrix in this expression is the one used by the POMPUS algorithm and E is a vector of experimental measurements:

$$(\mathbf{J}_p)_{ii,k} = \frac{\partial E_{ii}}{\partial s_k} \quad \text{and} \quad E = -(E_{11}, E_{22}, E_{33}, \dots, E_{pp})^T.$$

Breckon [5] has shown that, to a linear approximation, the change in the voltage measurement $v_{ij} = \langle M_i, R(\sigma_m) J_j \rangle$, Δv_{ij} , due to a conductivity change $\Delta \sigma = \sum \Delta s_k B_k = \Delta S \cdot B$ is

$$\Delta v_{ij} = - \int_{\partial \Omega} \left(\sum_k \Delta s_k B_k \right) \nabla \phi_i \cdot \nabla \phi_j = - \sum_K \Delta s_k \int_{\partial \Omega} B_k \nabla \phi_i \cdot \nabla \phi_j$$

where ϕ_i and ϕ_j are the potential fields induced in the conductivity distribution σ_m by boundary current densities M_i and J_j respectively. As the voltage measurement, v_{ij} , differs from the experimental measurement E_{ij} by a constant additive factor, the elements of the Jacobian matrix may be written:

$$(\mathbf{J}_p)_{ii,k} = \frac{\partial E_{ii}}{\partial s_k} = (\nabla_s E_{ii})_k^* = - \int_{\partial \Omega} B_k \nabla \phi_i \cdot \nabla \phi_i.$$

5.2. The POMPUS direction

The POMPUS direction, that is the direction of the POMPUS update, is defined by the least-squares system:

$$\Delta s = -\mathbf{J}_p^*(\mathbf{J}_p\mathbf{J}_p^* + \mu^2 I)^{-1} \mathbf{E}.$$

The angle, ω , between the POMPUS update and the steepest descent direction satisfies

$$\cos(\omega) = \frac{\Delta s \cdot \mathbf{Z}}{\|\Delta s\| \|\mathbf{Z}\|}. \quad (6)$$

The denominator of this expression is positive as it is the product of the norms of two vectors. The numerator may be rewritten:

$$\begin{aligned} \Delta s \cdot \mathbf{Z} &= \Delta s^* \mathbf{Z} = (-\mathbf{J}_p^*(\mathbf{J}_p\mathbf{J}_p^* + \mu^2 I)^{-1} \mathbf{E})^* (-2\mathbf{J}_p^* \mathbf{E}) \\ &= 2\mathbf{E}^* ((\mathbf{J}_p\mathbf{J}_p^* + \mu^2 I)^{-1})^* \mathbf{J}_p\mathbf{J}_p^* \mathbf{E} \\ &= 2\mathbf{E}^* (I + \mu^2(\mathbf{J}_p\mathbf{J}_p^*)^{-1})^{-1} \mathbf{E}. \end{aligned}$$

Thus $\Delta s \cdot \mathbf{Z} \geq 0$, since the eigenvalues of the symmetric matrix $(I + \mu^2(\mathbf{J}_p\mathbf{J}_p^*)^{-1})^{-1}$ are all non-negative. The condition that $\cos(\omega) \geq 0$ implies that the angle between the POMPUS update direction and the steepest descent direction $|\omega| \leq 90^\circ$. Thus the POMPUS update must decrease the Frobenius norm of D if the size of the update is sufficiently small. In practice the conductivity update is $\Delta s \cdot \mathbf{B}$ unless this results in an increase in the norm of D in which case a smaller step can be made or the Tikhonov factor can be increased.

For the unregularized case, $\mu = 0$, equation (6) can be written:

$$\cos(\omega) \geq \frac{2\|\mathbf{E}\|^2}{2\|\mathbf{E}\|^2 \sqrt{K(\mathbf{J}_p\mathbf{J}_p^*)}} = \frac{1}{K(\mathbf{J}_p)}$$

where $K(\mathbf{J}_p)$ is the condition number of the matrix \mathbf{J}_p . Thus the POMPUS direction diverges from the steepest descent direction as the Jacobian matrix becomes more ill conditioned. As the Tikhonov factor is increased the POMPUS direction converges to the steepest descent direction. As $\mu \rightarrow \infty$

$$-\mathbf{J}_p^T (\mathbf{J}_p\mathbf{J}_p^T + \mu^2 I)^{-1} \mathbf{E} = -\frac{1}{\mu^2} \mathbf{J}_p^T \mathbf{E} + \mathcal{O}\left(\frac{1}{\mu^4}\right).$$

Thus, the POMPUS update is always in a descent direction and Fletcher's result holds.

6. Experimental results

In this section two reconstruction algorithms are compared. RECON is a full matrix reconstruction algorithm based on trigonometric current and measurement patterns. Due to the constraints of our system a variant of POMPUS was used which applied trigonometric current patterns but used optimal measurement patterns. We would expect this algorithm to be less effective than POMPUS as the Frobenius norm of the transfer impedance operator is no longer determined only by the diagonal elements.

Table 1. A comparison of the execution times, in seconds, of the stages in a single iteration of RECON and POMPUS.

	RECON	POMPUS
Calculate the M and J matrices		2.03
Forward modelling		
Calculate system matrix	1.25	1.25
Solve finite element system	14.2	11.3
Calculate conductivity update		
C1MESH		
Construct least-squares system	212	6.72
Solve least-squares system	3.18	0.04
C2MESH		
Construct least-squares system	565	9.02
Solve least-squares system	203	0.04

In each case synthetic data were calculated from a finite element model for 20 current patterns. The region to be imaged was circular and driven by 32, symmetrically placed electrodes covering 50% of the boundary. Voltage measurements were made on point electrodes placed mid-way between current driving electrodes. Synthetic voltage data was calculated using a finite element model with 1157 nodes. The reconstruction used a finite element model of 761 nodes. RECON used 31 Fourier components of each voltage pattern as data for reconstruction. POMPUS used the one optimal measurement.

In table 1 the execution times of different stages in a single iteration of RECON and POMPUS are compared. POMPUS requires the calculation of the optimal experiments defined by the matrices M and J . This can be achieved by a singular value decomposition of the relatively small matrix D . Performing a SVD on an $n \times n$ matrix takes $O(n^3)$ operations which could be significant if a large number of experimental measurements were to be used for reconstruction. Typically this is unnecessary and reconstruction can be based on a small number of experiments using the most significant current patterns. Both algorithms require the calculation of a forward model, using the present 'best estimate' conductivity distribution, to predict the voltage measurements that will be made on the experimental region. This is accomplished in two stages: first a finite element system stiffness matrix is constructed and, second, the finite element system is solved for a number of right-hand sides corresponding to the number of experimental measurements used for reconstruction. The time required to solve the finite element system is dominated by factorization of the system stiffness matrix and relatively independent of the number of right-hand sides. For this reason POMPUS requires slightly less time than RECON for this stage as fewer experimental measurements are needed for reconstruction. The second stage of reconstruction involves the construction and solution of the least-squares system to calculate the conductivity update. For RECON this requires the construction and factorization of a matrix of dimension equal to the number of conductivity parameters in the image while for POMPUS a much smaller matrix of dimension equal to the number of experimental measurements used for reconstruction. The times required for this stage with two different conductivity parametrizations are shown. C1MESH has 93 conductivity parameters while C2MESH has 381 conductivity parameters. These times clearly show the computational advantages of the POMPUS algorithm especially where higher resolution images are to be calculated.

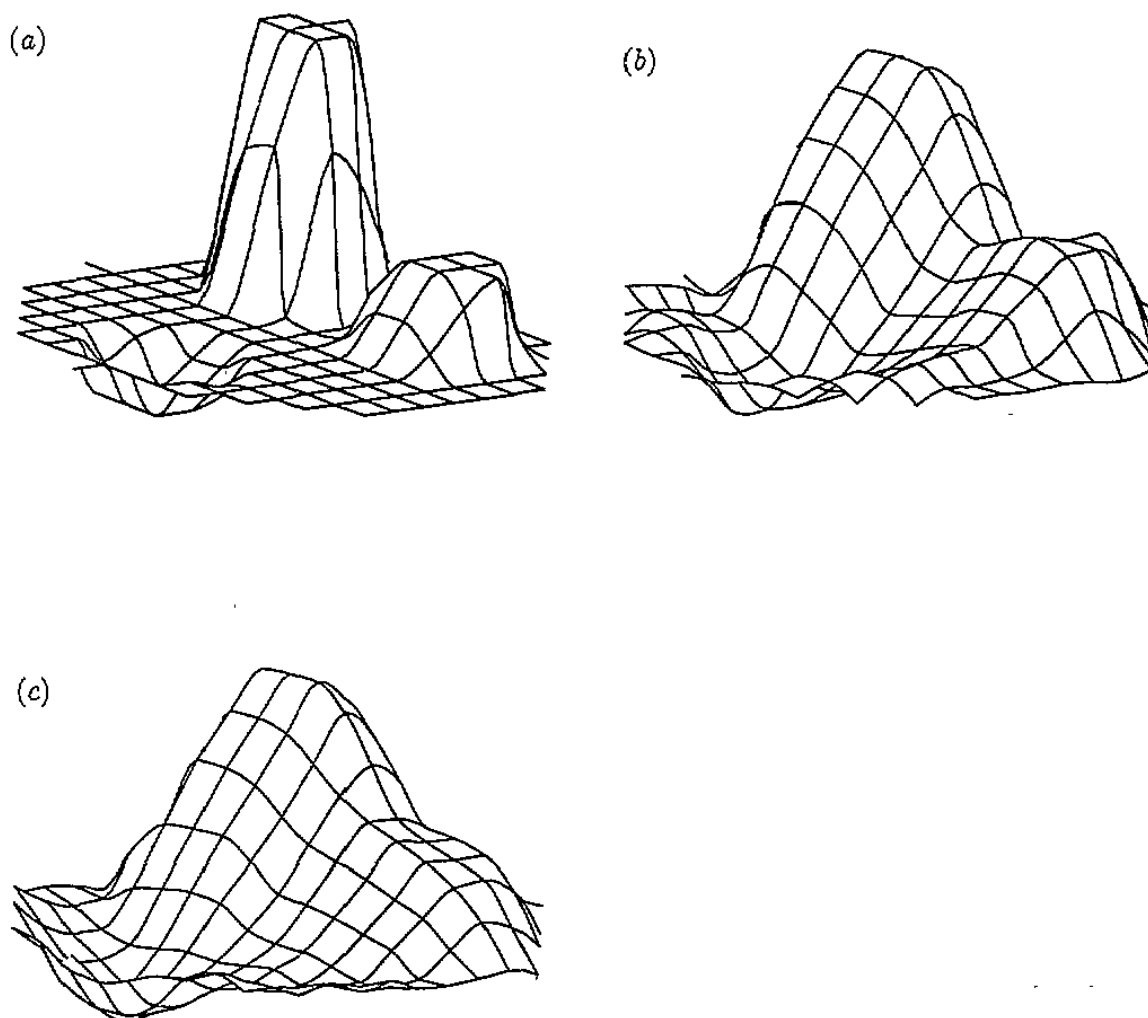


Figure 1. The reconstructed images of a uniform disk of radius 15 cm with three sub-regions of radius 4 cm and conductivity contrasts of 0.5, 2.0 and 4.0, image 1(a). Image 1(b) was produced after five iterations of RECON and image 1(c) after seven iterations of POMPUS.

Figure 1 compares reconstructions produced by RECON and POMPUS for a region with a complicated conductivity field. The imaged region is circular with three circular sub-regions with conductivity contrasts of 0.5, 2.0 and 4.0. These regions are clearly distinguished by both POMPUS and RECON although RECON shows higher resolution. It is perhaps surprising that the inferior variant of the POMPUS algorithm that we used performed as well as it did.

In figure 2 the convergence of RECON and POMPUS are compared as a function of iteration. RECON generally achieves more than POMPUS with each iteration but a RECON iteration requires considerably more computation. For the images in figure 1, RECON required approximately fifteen times the computation of POMPUS. A fast reconstruction algorithm could be constructed using several iterations of POMPUS as a pre-processor to RECON.

7. Conclusion

POMPUS can quickly locate conductivities close to the required image with considerably less

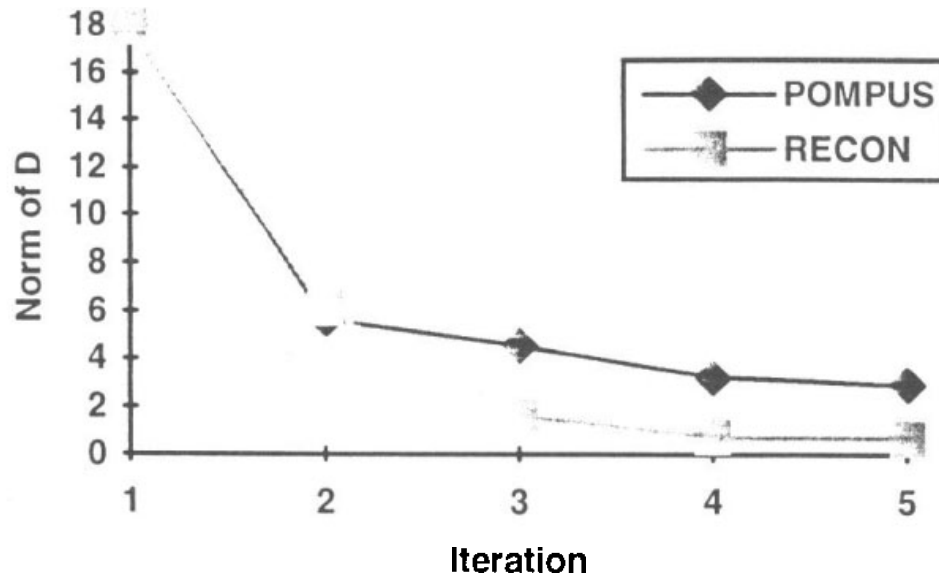


Figure 2. The convergence of RECON and POMPUS as a function of iteration. The distance from the ideal image is measured by the Frobenius norm of the difference in the model and experimental transfer impedance operators $\|D(\sigma_m)\|_F$.

calculation than algorithms previously used. It has massively reduced the computational effort required to calculate the conductivity update. The speed of forward modelling is now the limiting factor in the speed of multi-iteration, reconstruction algorithms. The use of POMPUS will greatly reduce one of the barriers presently hindering research into three-dimensional EIT imaging.

References

- [1] Barber D C and Brown B 1986 Recent developments in applied potential tomography-APT *Information Processing in Medical Imaging* ed S L Bacharach and Martinus Nijhoff, pp 106–21
- [2] Barber D C and Brown B 1990 Reconstruction of impedance images using filtered back-projection *Proc. Conf. on Electrical Impedance Tomography (Copenhagen 14th–16th) European Community Concerted Action on Electrical Impedance Tomography* pp 1–8
- [3] Breckon W R and Pidcock M K 1988 Some mathematical aspects of electrical impedance tomography *Mathematics and Computer Science in Medical Imaging (NATO ASI Series, F39)* ed M A Viergever and A E Todd-Pokropek (Berlin: Springer) pp 351–62
- [4] Breckon W R and Pidcock M K 1988 Data errors and reconstruction algorithms in electrical impedance tomography *Clin. Phys. Physiol. Meas.* **9** Suppl. A, 51–8
- [5] Breckon W R 1990 Image reconstruction in electrical impedance tomography *PhD Thesis* Oxford Polytechnic
- [6] Cheng K, Isaacson D, Newell J C and Gisser D G 1989 Electrode models for electric current computed tomography *IEEE Trans. on Biomedical Engineering* **36** 918–24
- [7] Fletcher R 1987 *Practical Methods of Optimisation* 2nd edn (New York: Wiley)
- [8] Folland G B 1976 *Introduction to Partial Differential Equations* (Princeton, NJ: Princeton University Press)
- [9] Golub G H and Van Loan C F 1983 *Matrix Computations* (Oxford: Johns Hopkins University Press)
- [10] Groetsch C W 1984 *The Theory of Tikhonov Regularisation for Fredholm Equations of the First Kind (Research Notes in Mathematics)* (London: Pitman)
- [11] Horn R A and Johnson C R 1985 *Matrix Analysis* (Cambridge: Cambridge University Press)
- [12] Isaacson D 1986 Distinguishabilities of conductivities by electric current computed tomography *IEEE Trans. Medical Imaging* **MI-5** 91–5
- [13] Paulson K S, Breckon W R and Pidcock M K 1992 Electrode modelling in electrical impedance tomography *SIAM J. Appl. Math.* **52** 1012–22
- [14] Paulson K S, Breckon W R and Pidcock M K 1992 A hybrid phantom for electrical impedance tomography *Clinical Phys. Physiol. Meas.* **13** Suppl. A, 155–61

- [15] Paulson K S, Lionheart W R B and Pidcock M K 1993 Optimal experiments in electrical impedance tomography *IEEE Trans. on Medical Imaging* **12** 681–6
- [16] Somersalo E, Cheney M and Isaacson D 1992 Existence and uniqueness for electrode models for electric current computed tomography *SIAM J. Appl. Math.* **52** 1023–40